# Mechanical Behavior of Circular Concrete Filled Steel Tube Column under Axial Loading for Sustainable Building

[1] A.K. Tiwary and [2]Ashok Kumar Gupta

[1]Department of Civil Engineering, Chandigarh University, Mohali, India.
E-mail: aditya.civil@cumail.in
[2]Professor, Department of Civil Engineering, Jaypee University of Information Technology, Solan, India.
E-mail: ashok.gupta@juit.ac.in

## Abstract

This paper presents an exploratory evaluation of the CFST columns under axial loading with different thicknesses of outer steel tube and column diameters. 4 mm and 5 mm outer steel tube with 100 mm, 125 mm, 150 mm outer diameter, and concrete of grade M30 was used in this study. The systematic outcomes are validated with the corresponding investigational by comparing its ductility index, secant stiffness, maximum confining pressure, and load-deformation behavior under axial loading on CFST columns. Many schemes were generated to evaluate the best set of parameters under axial loading to get the behavior of CFST columns. After studying the various increments of loading, the concrete began to fail from the center of the longitudinal section. This failure ends up at each end of the longitudinal section. This load transfer can resume from the middle of the longitudinal section. At this time the concrete begins to skinny from the middle and also the tension within the steel tube is targeted within the center of the longitudinal section. The load versus displacement graph is designed to evaluate the performance of the CFST column under axial loading.

**Keywords:** CFST columns, experimental investigation, finite element modeling, secant stiffness, confining pressure, ductility index.

# 1 Introduction

CFST is considered the main cross-sectional type of composite columns. Historically, encroaching on concrete in the previous type of column has been considered a protection against steel corrosion and fire [1, 2, 3]. Nowadays, longitudinal and lateral strengthening was included with the concrete encasement, and the potency caused due to the contact among the surrounding concrete and embedded steel tube was deployed for structural uses. On the other hand, CFST columns are made by releasing concrete in hollow steel tubes. Steel tube helps in situ concrete filling and thus eliminates the need for more formwork and leads to faster construction [4- 8]. Further, it does not require additional support. Therefore, CFST columns have been widely used as columns in both large span buildings [2] and high and medium rise buildings [3] and piers [9, 10]. As land availability is limited, large numbers of people need structures to support various activities. In previous studies, ductility improved by confining concrete and the two methods for providing confinement to concrete active confinement and passive confinement[11, 17]. First, confining stress is not binding unless the transverse reinforcement gap is reduced [16]. Second, the effect of deformation in concrete is introduced by the bending action in transverse reinforcement. The bending stress decreases with increasing distance from the bend [12]. In previous studies in [12, 13,14,15] CFST was found that CFST performs better than conventional RCC construction. In CFST, the steel tube also serves as a permanent formwork, and neglecting to strengthen the bar reduces construction time and costs. The limited pressure on the concrete core produced by the steel tube delays the formation of micro-cracks and reduces the splitting crack width [22].

Under tensile stresses to the CFST columns steel has the potential to show more stress than concrete, for this reason, research has been conducted to evaluate the effect of debonding on CFST, and conclude that the local buckling phenomenon in the circular steel tube in the debonding model is more severe than the sample devoid of debonding [17][18,19,20].

Steel tubes in the CFST only provide confinement to the concrete core by reversing the lateral stress. The stresses that arise depend on the lateral stresses and the lateral stresses in the specimen, which are turbulent. This makes it difficult to determine the amount of lateral stress and shear stress [11]. Equivalent stress umption is exemplified in models with two small major axes per axial load without surgical steel tube abnormalities [21, 24, 25][26,27],[30-33]. In the case of the CFST model with square and rectangular cross-sections, the arching action in the corners is not uniform stress in conventional RCC systems such as buckling between centre and edges.

## 2   Methodology

### *2.1 Test Specimens*

To examine the behavior of the CFST column under axial loading, a total of twelve composite (6 greased and 6 non-greased) specimens were cast. The specifications of the specimens are given in Table 1. The CFST columns of different sizes and the thicknesses of the steel tubes are shown in Fig. 1. For the preparation of greased specimens, grease was applied to the inner surface of the outer steel tubes. The casting of specimens was done in five layers, with each layer compacted using vibrator. CFST columns after casting are shown in Fig. 1.
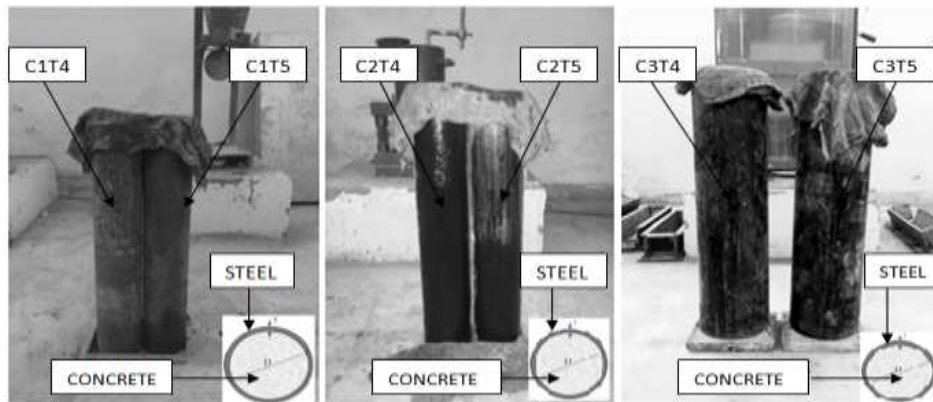


**Figure 1:** CFST Composite Columns

**Table 1** Geometry of Circular Steel Tubes Column

| Spe cim ens | Diam eter (mm) | Thic kness of steel( mm) | Hei ght (m m) | D/T | L/ D | Yield streng th of steel (MPa) | Com press ive stren gth of conc rete (MP a) | Area (mm²) | | |
|---|---|---|---|---|---|---|---|---|---|---|
| | | | | | | | | Steel (As) | Conc rete (Ac) | Tot al |
| C1 T4 | 100 | 4 | 600 | 25.0 | 6. 0 | 288 | 36.7 | 1206 | 7235 | 844 1 |
| C1 T5 | 100 | 5 | 600 | 20.0 | 6. 0 | 288 | 36.7 | 1492 | 7085 | 857 7 |
| C2 T4 | 125 | 4 | 600 | 31.3 | 4. 8 | 380 | 36.7 | 1521 | 1149 3 | 130 14 |
| C2 T5 | 125 | 5 | 600 | 25.0 | 4. 8 | 380 | 36.7 | 1885 | 1130 4 | 131 89 |
| C3 T4 | 150 | 4 | 600 | 37.5 | 4. 0 | 440 | 36.7 | 1835 | 1673 3 | 185 68 |
| C3 T5 | 150 | 5 | 600 | 30.0 | 4. 0 | 440 | 36.7 | 2278 | 1650 4 | 187 82 |

### 2.2 Test Setup and Measurement

A schematic outline of the specimen is represented in Fig. 2. An UTM machine HTP-2000 of capacity 2000 kN was utilized for the application of axial loading on the top of the specimens. The axial load was applied on the top surface of the specimens as presented in Fig. 2. For the evaluation of the experimental results, six specimens were cast after the inner coating of grease and other six specimens were cast without inner coating of grease. The behavior of greased and non-greased specimens was evaluated after 28 days.
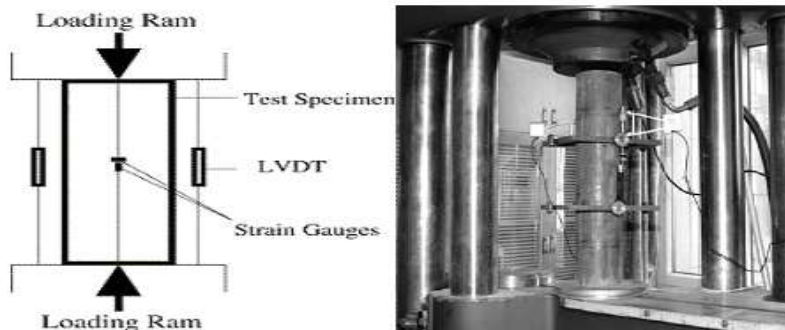


**Figure 2** Schematic Diagram of Test Arrangement

### 2.3 Experimental Analysis

In this paper, the performance of axially loaded CFST columns namely, C1T4, C1T5, C2T4, C2T5, C3T4 and C3T5 was investigated. The results observed from the experimental analysis were compared in terms of maximum load carried by the columns, load-deflection behaviour, ductility index, secant stiffness and maximum confining pressure for all the greased and non-greased specimens. The results obtained from experiment were compared to the simulated results and listed in Table 2.

**Table 2** Evaluation on Loading Capability of Greased and Non-Greased Columns

| Specimens | Load Carried by Column (kN) | | | | Peak Stress in Greased Column (MPa) | Simulated load capacity (kN) | Peak Stress in Non-Greased Column (MPa) |
|---|---|---|---|---|---|---|---|
| | Greased Column, $P_{GC}$ | Non-Greased Column, $P_{NGC}$ | % Increase in load | $P_{NGC}/P_{Gc}$ | | | |
| C1T4 | 823 | 834 | 1.3 | 1.01 | 97.5 | 843 | 98.8 |
| C1T5 | 827 | 836 | 1.1 | 1.01 | 96.4 | 849 | 97.5 |
| C2T4 | 1240 | 1252 | 1.0 | 1.00 | 95.3 | 1261 | 96.2 |
| C2T5 | 1248 | 1263 | 1.2 | 1.01 | 94.6 | 1268 | 95.8 |
| C3T4 | 1714 | 1749 | 2.0 | 1.02 | 92.3 | 1756 | 94.2 |
| C3T5 | 1721 | 1768 | 2.7 | 1.03 | 91.6 | 1774 | 94.1 |

## 3 Finite Element Modeling

The simulation technique to examine the behavior of CFST specimens is a compelling way to decrease money and time on additional analysis. The literatures on finite element analysis of circular CFST specimens are less. In this study, the numerical modeling of the specimens was considered to resolve these issues.

### 3.1 Description of FE Modeling

CFST is made of a visually filled steel tube with reference nodes with two upper and lower rigid panels.

### 3.1.1 Element Types

The most ordinarily used components for modeling is C3D4, C3D6 and C3D8. Of these components have 3 translation degrees of freedom (DOF) at every node. Consequently, C3D4 and C3D6 converge properly and need a fine mesh that consumes a great deal of your time. Therefore, C3D8 is most well-liked over C3D4 and C3D6 components for a solid continuous body [16]. The C3D8R element is also used for the concrete core. Due to time constraints, the mesh size is 20 mm. According to the literature, the best mesh available is the most accurate results, while a thicker mesh of 20 mm gives acceptable results. The Meshing of steel tube and concrete core is presented in Fig. 3.
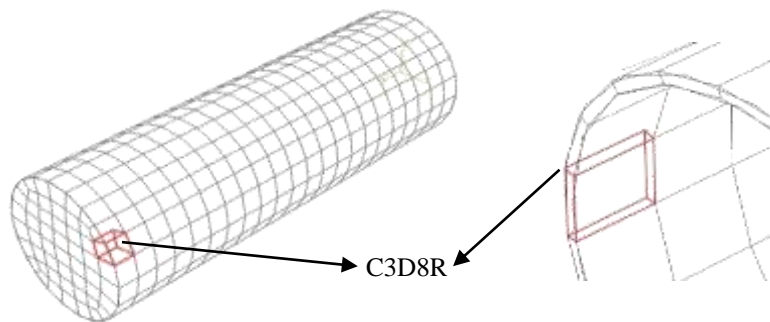
**Figure 3** Meshing of CFST Column with C3D8R Element

### 3.2 Material Modeling

### 3.2.1 Steel

For simplicity, the ideal trilinear stress-strain curve for steel was used. First, the elasticity of the steel extends along with the modulus to the yield point with a slope. The second part is the nature of plastic, which is stable under yield stress. The ideal trilinear stress-strain curve for steel is given by Fig. 4.

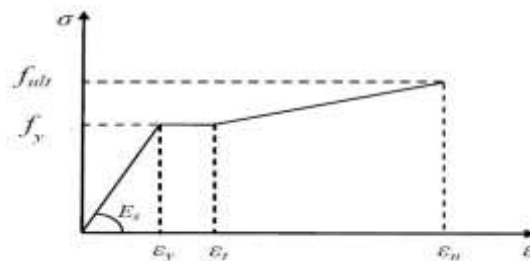$$\varepsilon_t = 10\varepsilon_y \tag{1}$$

**Figure 4** Idealized Trilinear Stress Strain Curve For Steel

### 3.2.2 Concrete

The stress-strain curve of concrete is calculated using the formula given by ACI (1999) with Young's modulus Ec.

$$E_c = 4700\sqrt{f_{cc}} \qquad (2)$$

Where $f_{cc}$ is calculated by means of relations [23]. The stress strain curve of confined and unconfined concrete is specified by Fig. 5.

$$f_{cc} = f_c + k_1 f_1 \qquad (3)$$

$$\varepsilon_{cc} = \varepsilon'_c \left(1 + K_2 \frac{f_1}{f_2}\right) \qquad (4)$$

Where, $k_1$ and $k_2$ denotes the constants that could be assumed as 4.1 and 20.5 correspondingly [24, 27].

$$\frac{f_1}{f_y} = 0.043646 - 0.000832 \left(\frac{d}{t}\right) \qquad \text{For } 21.7 \leq d/t \leq 47$$

(5)

$$\frac{f_1}{f_y} = 0.006241 - 0.0000357 \left(\frac{d}{t}\right) \qquad \text{For } 47 \leq d/t \leq 150$$
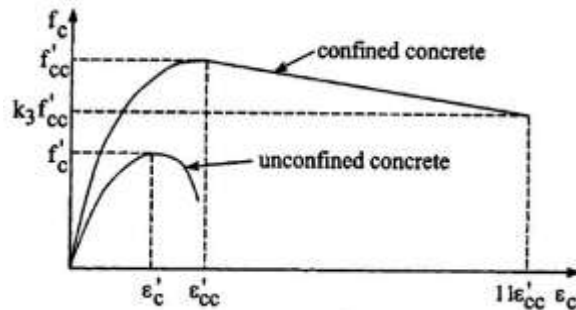
(6)



**Figure 5** Stress Strain Curve for Concrete

### 3.3 Validation of Results

The analytical results were separated with experimental results relating to load-deformation curves, ductility index, securitized rigidity and maximum limit stress of grease and non-grease specimens. The failure of the test specimens and numerical models were seen after the testing and simulation are shown in Fig. 6 and Fig. 7. The load-deformation performance curves of the CFST columns were observed by experiment for the grease and non-grease specimens as shown in Fig. 8, Fig. 9 and Fig. 10. The load-deformation behavior of the CFST columns observed by experimental and numerical modeling for nonlinear models is presented in Fig. 11, Fig. 12 and Fig. 13. The results showed that numerical modeling is in the observed load-deformation behavior great deal with exploratory values. The variability of the results between experimental and analytical analyzes stems from

differences in physical property and errors between test models and finite element models.



**Figure 6** Failure Mode of CFST Circular Columns Under Axial Loading
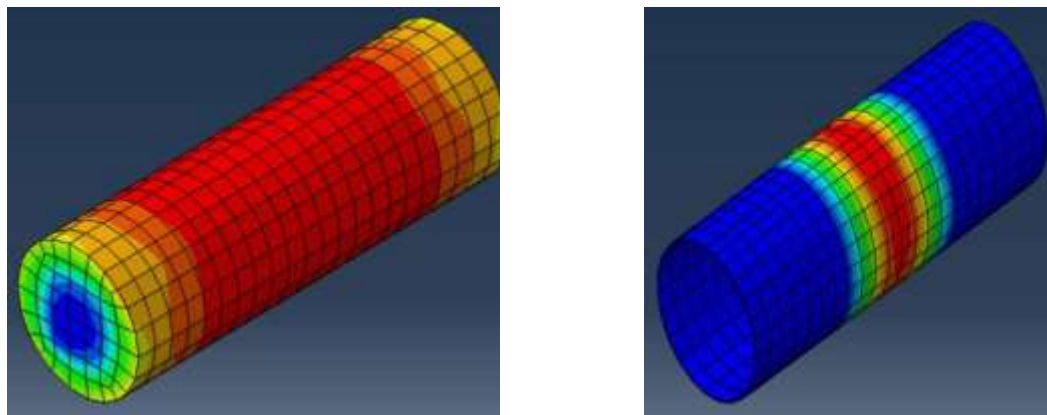


**Figure 7** Failure Location of Concrete and Steel Under Composite Loading

## 4 Results and Discussion

### *4.1 Axial Load-Deformation Curve of Greased and Non-Greased Specimens*

The comparison between load-deformation curves of the axial loaded greased and non-greased specimens C1T4, C1T5, C2T4, C2T5, C3T4, and C3T5 are presented in Fig. 8, Fig. 9 and Fig. 10. The observed experimental and analytical result of the specimens showed that the load-deformation behavior is nearer to one another. The slope of load-deformation curves of greased and non-greased specimens are almost the same but with the increase of composite loading, there is a slightly difference between the load-deformation behavior of the greased and non-greased columns. The elastic axial load bearing capacity of non-greased columns are slightly greater than the greased columns. The ratio of $P_{NGC}$ and $P_{GC}$ is found to vary from 1.00 to 1.03 for axial loaded columns. This shows that impact of contraction on the loading capability of CFST columns is relatively irrelevant.
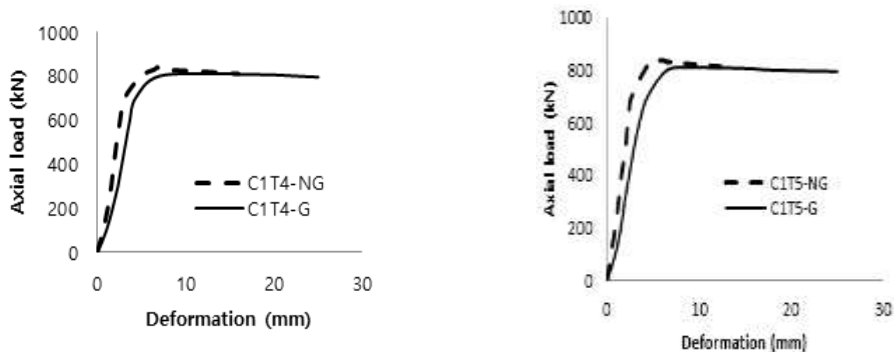


**Figure 8** Load-Deformation Curves For C1T4 And C1T5 Greased And Non-Greased Specimens
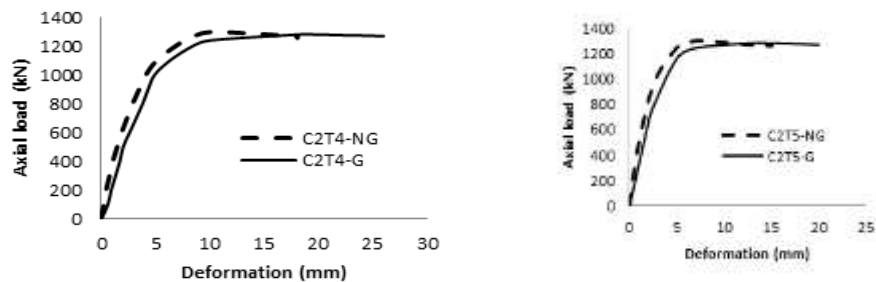


**Figure 9** Load-Deformation Curves For C2T4 And C2T5 Greased And Non-Greased Specimens
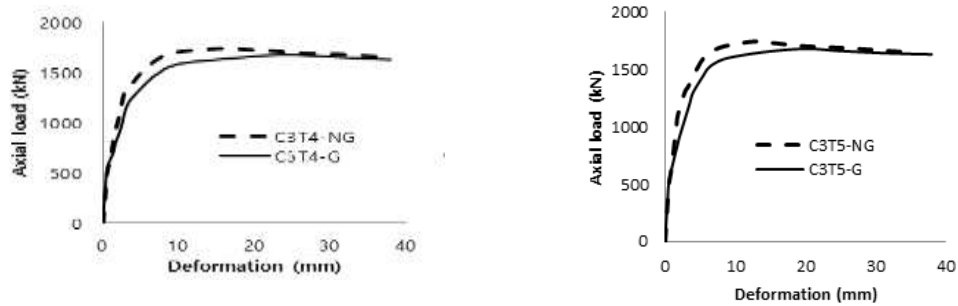
**Figure 10** Load-deformation curves for C3T4 and C3T5
greased and non-greased specimens

## 4.2 Experimental Vs. Simulated Axial Load-Deflection Curve

The load-deformation curves comparison between experimental and analytical results for specimens C1T4, C1T5, C2T4, C2T5, C3T4 and C3T5 are presented in Fig. 11, Fig. 12 and Fig. 13. The diversity of experimental and analytical results stems from the difference between physical property, test models and finite element models.
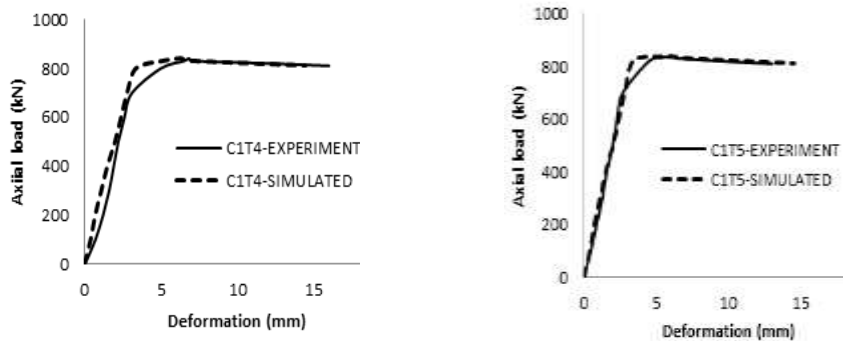


**Figure 11** Comparison of load-deformation curve for non-greased C1T4 and C1T5 column
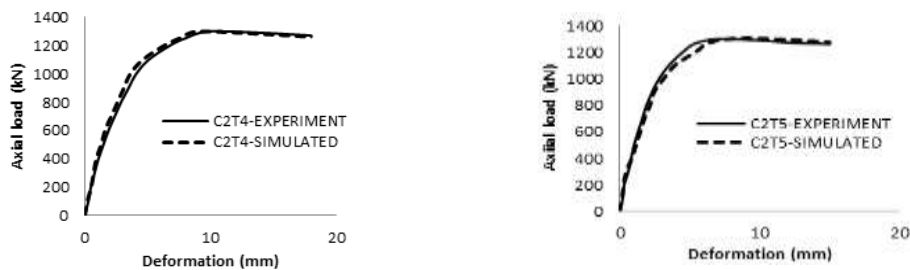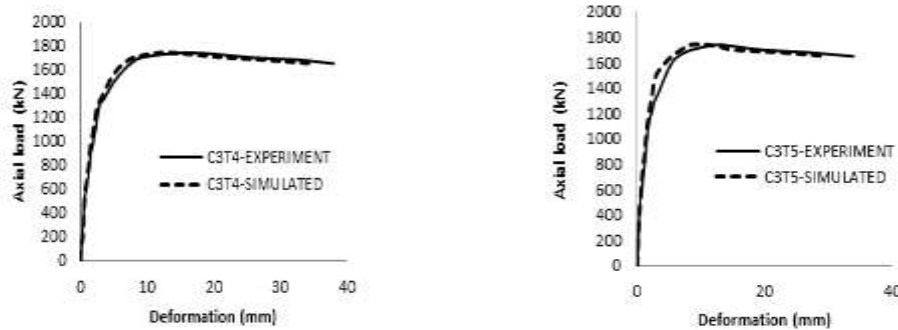


**Figure 12** Comparison of load-deformation curve for non-greased C2T4 and C2T5 column

**Figure 13** Comparison of load-deformation curve for non-greased C3T4 and C3T5 column
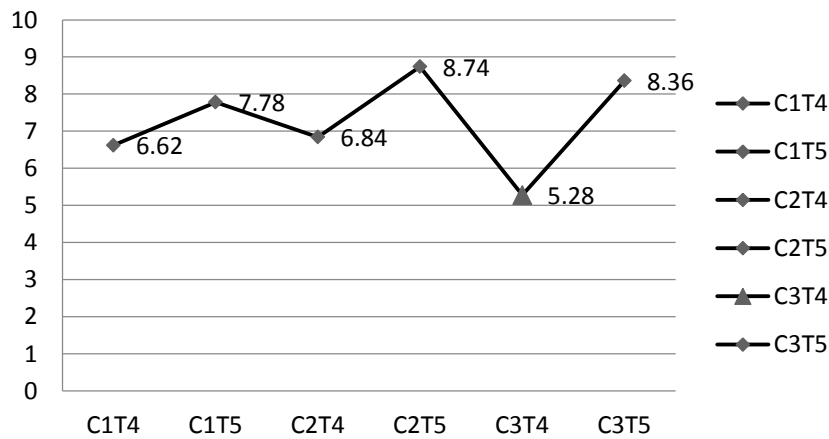
## 4.3 Maximum Confining Pressure ($F_{cp-Max}$)

The CFST members owe their unique properties to the radial confining pressure applied on concrete by steel tube that improves the ductility and compressive strength of concrete. Estimating the correct value of this parameter is pivotal to finding the load resistance of CFST member under any given type of loading. The experimental measurement of the value of confining pressure at any section is very difficult and required sophisticated equipment. Hence, the FEM model has been used to study its variations along with the height and the circumference of the specimens. Fig. 14 demonstrates the confining pressure distribution for the specimen was observed at an interval of 60 mm throughout height from the top of column specimens. The confining pressures of all specimens at the height of 60 mm from the top supports are shown in Fig. 15. The $f_{cp-max}$ of non-greased CFST columns is given by Table 3.



Maximum contact pressure at top surface of concrete and steel
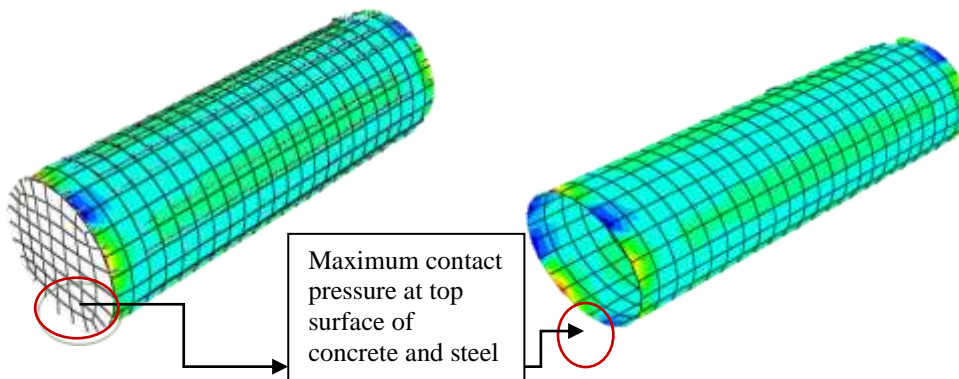
**Figure 14** Contact Pressure at Surface Node in Concrete And Steel

**Table 3** Maximum Confining Pressure of Non-Greased CFST Columns

| Specimens | Maximum confining Pressure $(f_{cp\text{-}max})$, $N/mm^2$ |
|-----------|--------------------------------------------------------------|
| C1T4 | 6.6 |
| C1T5 | 7.8 |
| C2T4 | 6.8 |
| C2T5 | 8.7 |
| C3T4 | 5.3 |
| C3T5 | 8.4 |



**Figure 15** Maximum Confining Pressure of Non-Greased CFST Columns

### 4.4 Secant Stiffness and Ductility Index for Greased and Non-Greased Columns

Secant stiffness is obtained by "ratio of ultimate compressive load to the displacement at an ultimate compressive load". The obtained outcomes point out that the secant stiffness decreases for the greased specimens as compare to the non-greased specimens. The greased and non-greased specimen C1T4 and C1T5 loses secant stiffness ranging from 41% to 59%. The greased and non-greased specimen C2T4 and C2T5 loses secant stiffness ranging from 21% to 28%. The greased and non-greased specimen C3T4 and C3T5 loses secant stiffness ranging from 18% to 27% . The Ductility Index was obtained by an equation [28]. DI for greased specimens decreases as compare to non-greased specimens with t = 4 mm and 5 mm . This indicates that the non-greased specimens became more ductile under axial composite loading. Other researcher given in [29] determines the CFST column's ductility after the rise in fire exposure. The secent stiffness and

ductility index of greased and non-greased CFST columns is shown by Table 4.

**Table 4** Secent Stiffness and Ductility Index of Greased and Non-Greased CFST Columns

| Specimens | Secent Stiffness, (kN/mm) | | Ductility Index (DI) | |
|---|---|---|---|---|
| | Greased | Non-Greased | Greased | Non-greased |
| C1T4 | 50.6 | 123.5 | 1.0 | 1.1 |
| C1T5 | 90.0 | 151.8 | 1.2 | 1.2 |
| C2T4 | 124.0 | 156.5 | 1.6 | 2.1 |
| C2T5 | 166.4 | 229.6 | 1.5 | 1.9 |
| C3T4 | 71.4 | 87.5 | 1.2 | 1.5 |
| C3T5 | 86.1 | 117.9 | 1.4 | 1.6 |

## 5 Conclusions

The below conclusions were attained from the analytical and experimental studies are given:

• The Stresses of non-greased CFST columns is greater than greased columns due to good bond behavior in CFST columns.

• The axial loading capability of non-greased columns is slightly higher than greased columns due to a lack of bonding behavior between concrete and steel.

• The secant stiffness of non-greased CFST columns is greater than greased columns. The secant stiffness of greased and non-greased specimens is ranging from 18% to 59% and it is seen that C2T5 non-greased specimen has higher secant stiffness.

• The ductility index of non-greased columns is slightly higher than the greased columns. This means that the non-greased specimens have more ductility as compared to the greased specimens.

• The confining pressure given by steel tube to concrete is generally emphasized near the columns ends by friction due to the machine loading plate and CFST top and bottom plates. The affected length of CFST columns is generally between 20 mm and 40 mm from either side. This results in very high compressive stresses in concrete in these areas.

## References

[1] M.-L. Wang, M. Liu, and F.-S. Zhu, "Mechanical properties of concrete-filled steel tube columns strengthened with CFRP under axial load after high temperature," Dongbei Daxue Xuebao/Journal Northeast. Univ., vol. 27, no. 12, pp. 1381–1384, 2006.

[2] A. Elremaily and A. Azizinamini, "Behavior of circular concrete-filled steel tube columns," in Proceedings of the Conference: Composite Construction in Steel and Concrete IV, pp. 573–583,2000.

[3] G.-C. Li, Z.-Q. Wang, and Y.-M. Shao, "Bearing capacity of gangue concrete filled steel tubular member under moment," Shenyang Jianzhu Daxue Xuebao (Ziran Kexue Ban)/Journal Shenyang Jianzhu Univ. Natural Sci., vol. 21, no. 6, pp. 654–657, 2005

[4] H.-L. Wu and Y.-F. Wang, "Study on size effect of concrete filled steel tubular columns," Harbin Gongye Daxue Xuebao/Journal Harbin Inst. Technol., vol. 39, no. SUPPL. 2, pp. 22–25, 2007

[5] L. Ling, C.-A. Tang, S.-H. Wang, and Z.-Z. Liang, "3D-numerical simulation on failure process of concrete-filled steel tube column," Dongbei Daxue Xuebao/Journal Northeast. Univ., vol. 29, no. 10, pp. 1505–1508, 2008,

[6] J. Nie, Y. Zhu, and J. Fan, "Experimental study on steel-concrete composite transfer frame," Jianzhu Jiegou Xuebao/Journal Build. Struct., vol. 30, no. 4, pp. 30–37, 2009.

[7] L. Wang, T. Zhao, and H. Li, "Experimental research and theoretical analysis of square steel tube columns filled with steel-reinforced high-strength concrete subjected to eccentric loading," Jianzhu Jiegou Xuebao/Journal Build. Struct., vol. 31, no. 7, pp. 64–71, 2010.

[8] E. Abdelgadir, J. Bohai, F. Zhongqiu, and H. Zhengqing, "The behavior of lightweight aggregate concrete filled steel tube columns under eccentric loading," Steel Compos. Struct., vol. 11, no. 6, pp. 469–488, 2011.

[9] Y. Xu, P. Sun, and L. Zhang, "Finite element analyze for a connection between steel reinforced concrete filled with steel tube column and steel beam," Adv. Mater. Res., vol. 243–249, pp. 51–54, 2011

[10] Z.-P. Chen, F. Liu, H.-H. Zheng, and J.-Y. Xue, "Research on the bearing capacity of recycled aggregate concrete-filled circle steel tube column under axial compression loading," in 2010 International Conference on Mechanic Automation and Control Engineering, (MACE2010), pp. 1198–1201,2010.

[11] Y. Xu, P. Sun, O. E. Sysoev, and D. Victo, "Finite element analysis on CFRP steel reinforced concrete filled with steel tube column under bidirectional eccentric load," Shenyang Jianzhu Daxue Xuebao (Ziran Kexue Ban)/Journal Shenyang Jianzhu Univ. Natural Sci., vol. 27, no. 6, pp. 1085–1092, 2011

[12] W. Cao, J. Zhang, X. Duan, H. Dong, and C. Yin, "Experimental study on mechanical performance of rectangular concrete filled steel tube columns under reciprocating tension and compression load," World Inf. Earthq. Eng., vol. 28, no. 2, pp. 1–7, 2012.

[13] J. Gao, Y. Wu, and J. Huo, "Experimental study on the hysteretic behaviors of thin-walled corrugated concrete-filled steel tube column," World Inf. Earthq. Eng., vol. 28, no. 3, pp. 34–42, 2012.

[14] Q.-X. Wang, S.-R. Liu, B.-J. Si, and G. Wang, "Mechanical behavior of concrete-filled steel tube column-steel beam joints with penetration steel bars under low cyclic loading," Dalian Ligong Daxue Xuebao/Journal Dalian Univ. Technol., vol. 52, no. 1, pp. 54–59, 2012.

[15] W. Gu, H.-N. Li, and G.-S. Sun, "Study on mechanical properties of damaged axially loaded concrete filled steel tube columns strengthened with CFRP composite materials," Jianzhu Cailiao Xuebao/Journal Build. Mater., vol. 16, no. 1, pp. 138–142, 2013

[16] M. Hou, L. Li, J. Dong, and Q. Wang, "Influence of amount of recycled coarse aggregate on mechanical properties of steel tube columns," Adv. Mater. Res., vol. 647, pp. 748–752, 2013

[17] G. C. Li, B. Zhou, and J. H. Pan, "Finite element analysis on concrete-filled square steel tube short columns with inner CFRP profiles under axial compression," Appl. Mech. Mater., vol. 578–579, pp. 335–339, 2014

[18] L. Fu, F.-X. Ding, L.-X. Gu, and Y.-Z. Gong, "Mechanical properties of stirrups confinement concrete-filled round-ended steel tubular stub short columns under axial compression," Huanan Ligong Daxue Xuebao/Journal South China Univ. Technol. (Natural Sci., vol. 42, no. 11, pp. 113–120, 2014

[19] Z. Yang and M. Chen, "Analysis on the impact behavior of super high strength concrete filled steel tube columns," Metall. Min. Ind., vol. 7, no. 12, pp. 6–11, 2015.

[20] H. Niu, W. Cao, H. Dong, and Z. Zhou, "Experimental research on highstrength recycled concrete-filled steel tube columns subjected to axial compression," Jianzhu Jiegou Xuebao/Journal Build. Struct., vol. 36, no. 6, pp. 128–136, 2015.

[21] Z.-P. Chen, X.-G. Zhang, J.-Y. Xue, and Y.-S. Su, "Experimental study on aseismic performance of frame constructed by recycled-concrete-filled-square- steel-tube columns and beams," Gongcheng Lixue/Engineering Mech., vol. 33, no. 8, pp. 32–38, 2016, doi: 10.6052/j.issn.1000-4750.2014.06.0501.

[22] J. S. S. Jegadesh and S. Jayalekshmi, "Using fibres and fly ash in concrete-filled steel tube columns," Proc. Inst. Civ. Eng. Struct. Build., vol. 169, no. 10, pp. 741–755, 2016.

[23] Z. C. Hao H., Ed., 24th Australasian Conference on the Mechanics of Structures and Materials, ACMSM 2016. CRC Press/Balkem, 2017.

[24] L.-H. Xu, M. Wu, P.-H. Zhou, Y.-S. Gu, and M.-Y. Xu, "Experimental investigation on high-strength self-stressing and self-compacting

concrete filled steel tube columns subjected to uniaxial compression," Gongcheng Lixue/Engineering Mech., vol. 34, no. 3, pp. 93–100, 2017

[25] W.-H. Wang, W. Zhang, Y. Bai, and Q.-H. Tan, "Axial performance of square concrete-filled steel tube (CFST) columns reinforced by circular steel tubes at elevated temperatures," Gongcheng Lixue/Engineering Mech., vol. 35, no. 3, pp. 141–150, 2018, doi: 10.6052/j.issn.1000-4750.2016.11.0884.

[26] C. Liu, Q. Li, Z. Lu, and H. Wu, "A review of the diagrid structural system for tall buildings," Struct. Des. Tall Spec. Build., vol. 27, no. 4, 2018.

[27] Y.-H. Wang, Y.-Y. Wang, and S.-W. Hu, "Study on the mechanical properties of CFRP circumferentially confined concrete filled steel tube column of marine structure under compression-bending-torsion combined load [海洋结构CFRP环向约束钢管混凝土柱在压弯扭荷载下的力学性能研究]," Gongcheng Lixue/Engineering Mech., vol. 36, no. 8, pp. 96–105, 2019.

[28] J. Xue, L. Ma, and J. Lin, "Lateral stiffness and ductility analysis on hybrid column of concrete filled square steel tube column and reinforced concrete circular column in traditional buildings [传统风格建筑方形CFST-圆形RC截面混合柱侧移刚度及延性分析]," Prog. Steel Build. Struct., vol. 21, no. 4, pp. 61–69, 2019.

[29] W. Hao, X. Xu, and Z. Niu, "Experimental study on the mechanical behavior of RPC filled square steel tube columns subjected to eccentric compression," Frat. ed Integrita Strutt., vol. 12, no. 46, pp. 391–399, 2018

[30] Y.-P. Wu, Z.-H. Chen, T. Zhou, X.-D. Chen, and X.-D. Wang, "Experimental and numerical studies on Seismic Performance of The SCFST Column Eccentrically Braced Frames," Adv. Struct. Eng., 2020,

[31] C. Avci-Karatas, "Prediction of ultimate load capacity of concrete-filled steel tube columns using multivariate adaptive regression splines (MARS)," Steel Compos. Struct., vol. 33, no. 4, pp. 583–594, 2019

[32] S. Fang, F. Liu, Z. Xiong, J. Fang, and L. Li, "Seismic performance of recycled aggregate concrete-filled glass fibre-reinforced polymer-steel composite tube columns," Constr. Build. Mater., vol. 225, pp. 997–1010, 2019

[33] M. Abhilash, S. Jhanjhari, P. Parthiban, and J. Karthikeyan, "Axial behaviour of semi-lightweight aggregate concrete-filled steel tube columns - A DOE approach," J. Constr. Steel Res., vol. 162, 2019.

**Biographies**



 **A.K. Tiwary,** Professor, Department of Civil Engineering, Chandigarh University, Mohali, India.



**Ashok Kumar Gupta,** Professor, Department of Civil Engineering, Jaypee University of Information Technology, Solan, India.